JKPK (Jurnal Kimia dan Pendidikan Kimia), *Vol. 10, No. 3, 2025* *Hal. 564-579*
Chemistry Education Study Program Universitas Sebelas Maret *ISSN 2503-4146*
http://jurnal.uns.ac.id/jkpk *ISSN 2503-4154 (online)*

Molecular Docking Analysis of Bioactive Compounds from *Jatropha Curcas* L. Leaves Against Lipoxygenase Inhibitors as Antioxidant Candidates

Fahmi Sadik [1]*, Wa Ode Rufiyani [1], Muhammad Fakhrur Rajih Hi. Yusuf [2]

[1]*Department of Pharmaceutical Biology, Pharmacy Study Program, Faculty of Medicine and Health Sciences, Universitas Khairun, Ternate, Indonesia*

[2]*Department of Pharmaceutical Pharmacology, Pharmacy Study Program, Faculty of Medicine and Health Sciences, Universitas Khairun, Ternate, Indonesia*

ABSTRACT

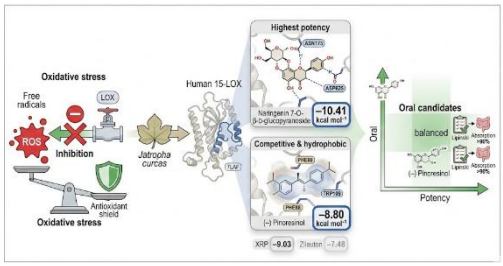

Oxidative stress results from an imbalance between reactive oxygen species (ROS) and the body's antioxidant defense system, contributing to various degenerative diseases. The enzyme Lipoxygenase (LOX) plays a crucial role in ROS formation; thus, its inhibition offers a strategic approach to mitigate oxidative damage. This study aims to evaluate the potential of bioactive compounds from *Jatropha curcas* L. leaves as LOX inhibitors using *in silico* approaches. The target protein (Human 15-LOX, PDB ID: 7LAF) and ligand structures were retrieved from the Protein Data Bank and PubChem. Flexible molecular docking simulations were performed using YASARA Structure to accommodate receptor side-chain adjustments, validated against the native ligand (XRP) and a positive control (Zileuton). The results revealed that Naringenin-7-O-β-D-glucopyranoside exhibited the strongest binding affinity (–10.41 kcal/mol), surpassing both the native ligand (–9.03 kcal/mol) and Zileuton (–7.48 kcal/mol), driven by extensive hydrogen bond networks with residues ASN173 and ASP625. Meanwhile, the aglycone (-)-Pinoresinol demonstrated competitive affinity (–8.80 kcal/mol) stabilized by hydrophobic interactions with PHE88 and TRP109. While glycosides showed superior potency, (-)-Pinoresinol and Epicatechin were identified as the most rational oral drug candidates, fulfilling Lipinski's Rule of Five and demonstrating high intestinal absorption (>90%) in ADMET analysis. These findings provide a structure-based rationale for selecting *J. curcas* metabolites as promising LOX inhibitor candidates for further *in vitro* validation.

Keywords: *Molecular docking; Jatropha curcas; Lipoxygenase; Antioxidant; Oxidative stress.*
**Corresponding Author:* *fahmisadik@unkhair.ac.id*
How to cite: F. Sadik, W. O. Rufiyani, and M. F. R. H. Yusuf, "Molecular Docking Analysis of Bioactive Compounds from *Jatropha Curcas* L. Leaves As Lipoxygenase Inhibitors and Antioxidant Candidates," *JKPK (Jurnal Kimia dan Pendidikan Kimia)*, vol. 10, no. 3, pp. 564-579, 2025. [Online]. Available: https://doi.org/10.20961/jkpk.v10i3.110639
Received: *2025-11-04* ***Accepted:*** *2025-12-12* ***Published:*** *2025-12-31*

INTRODUCTION

Oxidative stress, triggered by the accumulation of Reactive Oxygen Species (ROS) and Reactive Nitrogen Species (RNS), has the potential to induce biomolecular damage, ultimately leading to apoptosis, necrosis, and a range of cellular pathologies [1]. Within this biochemical pathway, the enzyme Lipoxygenase (LOX) assumes a pivotal role as a pro-oxidant, facilitating the oxidation of polyunsaturated fatty acids to hydroperoxide [2]. The catalytic function of LOX substantially contributes to the generation of reactive species that intensify

oxidative stress, inflammation, and carcinogenesis [2]. Consequently, inhibiting the activity of this enzyme emerges as a vital strategy for alleviating oxidative stress. Such a central role renders LOX a highly pertinent molecular target for in silico screening studies of natural inhibitors.

Antioxidants play a significant role in mitigating the detrimental effects of free radicals on biological and food systems [3]. Despite the demonstrated efficacy and cost-effectiveness of synthetic antioxidants such as Butylated Hydroxyanisole (BHA) and Butylated Hydroxytoluene (BHT), their application is increasingly curtailed by international food safety regulations [4]. Toxicological investigations indicate that prolonged exposure to these compounds may pose carcinogenic risks and induce mutagenesis [4]. The apprehensions surrounding the adverse effects of these synthetic agents have galvanized the scientific community to intensify the quest for natural antioxidant alternatives that exhibit comparable effectiveness while maintaining an improved safety profile.

Leaves of *Jatropha curcas* L. represent a promising source of natural antioxidant candidates due to their richness in secondary metabolites [5], with the ethanol extract of its leaves reported to exhibit robust antioxidant activity, evidenced by an IC50 value of 32.83 µg/mL in the DPPH free radical capture assay [6]. Furthermore, the leaves of this species possess a considerable total phenolic content, quantified at 56,659 µg GAE/g [7].

Flavonoid compounds within this botanical family are acknowledged for their substantial inhibitory activity against oxidoreductase enzymes, including Lipoxygenase (LOX) [8], typically via competitive interaction mechanisms or chelation formation [9]. It is this empirical substantiation of flavonoids' capacity as LOX inhibitors that renders them highly suitable candidates for further examination through computational methodologies.

Molecular docking is frequently employed to elucidate interaction mechanisms by predicting binding modes and binding affinities between phytochemical ligands and target macromolecules such as Lipoxygenase (LOX) enzymes [10]. While the antioxidant capacity of the crude extract of Jatropha curcas leaves has been extensively documented [11], to the best of our knowledge, data regarding the molecular interactions of its secondary metabolites specifically with the crystal structure of Human 15-Lipoxygenase (GDP ID: 7LAF) remain markedly limited.

This study aims to investigate the potential of selected bioactive compounds derived from *Jatropha curcas* L. leaves as antioxidants through molecular docking simulations against Lipoxygenase (LOX) enzymes, while also assessing their pharmacokinetic and toxicity profiles via ADMET prediction. The anticipated outcomes of this research are expected not only to bolster the utilization of local biological resources in the formulation of herbal medicines but also to furnish a structure-based rationale for identifying potential LOX inhibitor candidates from Jatropha curcas leaves prior to advancing to subsequent in vitro testing phases.

METHODS

1. Equipment and Materials

Computational analysis was conducted using a personal computing device running Windows 11 Pro (64-bit), equipped with an Intel Core i5 processor and 32 GB of RAM. The requisite macromolecular structures and ligand compounds were procured from the Protein Data Bank (PDB) and PubChem databases. Furthermore, the software employed for molecular modeling and simulation encompasses YASARA Applications and Discovery Studio Visualizer (DSV) 2025 Client v25.1.0. Subsequently, ADMET Analysis was executed utilizing the pkCSM web server.

The target protein used in this investigation is the crystallographic structure of Human 15-Lipoxygenase (PDB ID: 7LAF), which was obtained from the Protein Data Bank. Conversely, the chemical structures of the test ligand compounds were retrieved from the PubChem database in a two-dimensional data format. The test ligands comprised selected secondary metabolites derived from phytochemical analyses of *Jatropha curcas* L. [12]. The selection criteria were previously established based on the availability of structural data within the PubChem database, as well as the structural diversity that represents groups of flavonoids, lignans, and phenolic glycosides.

Zileuton® was incorporated as a positive control alongside the native ligand (XRP) to support comparative evaluation of binding activity [13]. The selected test compounds included Naringenin-7-O-β-D-glucopyranoside, Pinoresinol-4′-O-β-D-glucopyranoside, Buddlenol D, Isovitexin, Syringaresinol-4′-O-β-D-glucopyranoside, Chamaejasmin, (2S,3S)-Epicatechin, (2R,3R)-Dihydroquercetin, (2R,3S)-Catechin, (-)-Pinoresinol, Isoneochamaejasmin A, (-)-Syringaresinol, and Neochamaejasmin B.

2. Ligand Preparation

The preparation of ligands was meticulously executed to obtain a stable and representative molecular conformation prior to conducting molecular docking analyses against the Lipoxygenase enzyme (7LAF). All test compounds derived from the foliage of *Jatropha curcas* L. were effectively prepared and transformed into three-dimensional (3D) representations. The ligand structures were sourced from the PubChem database in SDF format. Subsequently, a comprehensive geometry optimization process was undertaken utilizing the YASARA Structure software. During this phase, an energy minimization experiment was conducted to refine the molecular geometry, rectify bond lengths and angles, and mitigate unnatural steric interactions, until the most thermodynamically stable 3D configuration was attained [14]. This optimization phase ensures that the entire set of test compounds possesses optimal structural integrity and suitable force field parameters prior to engagement with the enzyme active site in the tethering simulation [15].

3. Lipoxygenase Protein Preparation

Lipoxygenase proteins identified by PDB ID 7LAF were acquired from the Protein Data Bank and subsequently processed utilizing YASARA software. The initial phase of the preparation involves the meticulous

cleaning of the structural model, encompassing the elimination of non-essential crystallographic water molecules and the disassociation of the native ligand from the principal protein backbone. This particular stage is designed to streamline the simulation environment and mitigate solvent interference within the active site [16]. Visualization of the prepared Lipoxygenase structure is presented in Figure 1.

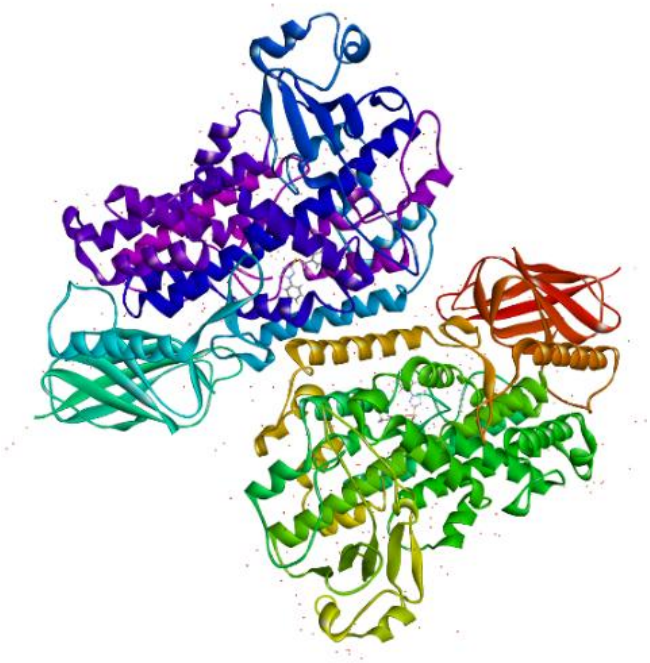

Figure 1. *Lipoxygenase* Protein (PDB ID: 7LAF)

The protein structure was then optimized to improve hydrogen atom orientation, residue protonation states, and tautomeric forms under physiological conditions at pH 7.4. Protonation assignment was performed to represent realistic ionization of titratable residues, including selection of appropriate histidine tautomers, while hydrogen atoms were refined to stabilize the hydrogen bonding network and minimize steric clashes. The AMBER03 force field parameters are subsequently applied automatically to assign atomic charges and potential energy parameters throughout the entire protein structure, eliminating the need for manual charge assignments. This refined protein structure was subsequently designated as a receptor for simulated docking.

4. Docking Method Validation

The validation process for the docking methodology is conducted to ascertain the precision of ligand positioning and the dependability of the employed simulation protocol. This validation is performed by executing a redocking simulation of the initial ligand (XRP) within the active site of the target protein. The parameters for the simulation, encompassing definitions of search space and tethering algorithms, are established to be identical to those employed

during the simulation phase of the test ligand (production run).

The tethering region (simulation cell) is delineated around the initial ligand with central coordinates of x = 106.44, y = 106.44, and z = 106.44, along with spatial dimensions of 90 x 90 x 90 Å, thereby encompassing the entirety of the active site residue. Simulations are conducted by configuring the number of repetitions (docking runs) to a total of 100 iterations. Upon the completion of the redocking process, the conformation exhibiting the lowest binding energy is selected and overlaid with the crystal structure of the original ligand to compute the Root Mean Square Deviation (RMSD) value. The validation procedure is deemed successful and valid if the resultant RMSD value is less than or equal to 2 Å [16].

5. Molecular docking

Molecular docking simulations were conducted employing tethering algorithms integrated within the YASARA Structure software [16]. In contrast to conventional methodologies that preserve the rigidity of receptors, this simulation adopts a flexible paradigm wherein the side chains of amino acid residues located at the active site are permitted to exhibit mobility (side-chain flexibility). This methodological framework is designed to encapsulate the influence of induced-fit modifications as ligands engage with proteins, thereby yielding more precise energy estimations.

Simulation parameters were defined by performing 100 docking iterations for each ligand to ensure thorough sampling of the conformational space, and all test compounds, including the native ligand (XRP) and the positive control (Zileuton), were docked using a chamber definition consistent with the validation stage. The resulting poses were ranked, and the conformation showing the lowest (most negative) binding energy alongside the most stable interaction geometry was selected as the optimal pose for subsequent molecular interaction analysis [17].

6. Drug-likeness evaluation with Lipinski's Rule of Five

The viability of the compound as a potential oral pharmacological agent was scrutinized through the lens of physicochemical attributes indicative of drug-likeness. The evaluative criteria encompassed Lipinski's Rule of Five, which includes parameters such as Molecular Weight, logP, Hydrogen Bond Donors, and Hydrogen Bond Acceptors, in addition to the supplementary metric of Molar Refractivity (40-130) [18]. This analytical process was conducted utilizing structural information derived from PubChem, which was processed via the SCFBIO web server at IITD (http://www.scfbio-iitd.res.in/software/drugdesign/lipinski.jsp). This particular stage of evaluation was implemented to determine the bioavailability characteristics of the test ligands, to prioritize compounds that not only exhibit a robust binding affinity to LOX but also meet the requisite criteria for being considered effective oral pharmaceuticals.

7. ADMET study using pkCSM

The pharmacokinetic characteristics and potential toxicity of the experimental compounds were predicted through in silico

methodologies utilizing the PKCSm web server [19]. The assessment was not confined to a finite set of specific parameters; instead, it concentrated on numerous pivotal ADMET descriptors, which included: human intestinal absorption, status as a substrate for P-glycoprotein, permeability across the blood-brain barrier, central nervous system (CNS) permeability, interactions with cytochrome P450 enzymes (CYP2D6 and CYP3A4), overall clearance, in addition to toxicity metrics such as mutagenicity (AMES assay) and hepatotoxicity. The quantitative data acquired are subsequently analyzed against the standard threshold values outlined in the literature for classifying the pharmacokinetic profiles of compounds as 'favorable' or 'less favorable' [20].

8. Visualization of Ligand-Protein Complexes

Molecular interaction analyses were conducted on ligand conformations exhibiting the highest binding affinity scores derived from docking simulation outcomes. The Discovery Studio Visualizer software was used to identify specific non-covalent interactions, including hydrogen bonding, hydrophobic interactions, electrostatic interactions, and π-π stacking. The results of the analysis are illustrated in a two-dimensional interaction diagram to elucidate the crucial amino acid residues involved, alongside three-dimensional visualizations to provide a spatial understanding of the ligand orientation within the active site of the target protein [21].

RESULTS AND DISCUSSION

1. Docking Method Validation

Preliminary structural examination of the Lipoxygenase protein complex (PDB ID: 7LAF) elucidated the orientation of the endogenous ligand (XRP) occupying deeply-seated hydrophobic binding pockets [22]. The identification of the crystallographic position of XRP delineates critical residues within the active site, which subsequently serve as a reference in the delineation of simulation space coordinates for the validation procedure.

The validation of the methodology was executed by simulating (redocking) the original ligand into the active site utilizing the YASARA protocol [16]. According to the analysis findings, an RMSD value of 1.913 Å was achieved (Table 1). The attainment of this value, which remains beneath the 2 Å validity threshold, signifies that the docking protocol employed possesses a high degree of geometric fidelity in reproducing crystallographic configurations [23]. In addition to the validity of geometry, this simulation yields a Binding Energy of -9.05 kcal/mol, as determined by the YASARA force field scoring function. This energy measurement is further established as a reference standard for evaluating the competitive efficacy of test compounds.

The illustration presented in Figure 2 depicts an exact overlay between the ligand obtained from redocking (represented in blue) and the initial ligand (depicted in green). Moreover, the analysis of interactions has substantiated that the redocking configuration effectively preserved the binding orientation towards critical residues

located at the active site, which encompasses significant interactions with PHE438 and GLU369. This consistency in both structural and chemical aspects validates the dependability of the computational methodology employed, thereby establishing a robust basis for predicting molecular interactions involving the test compounds derived from *Jatropha curcas* L. leaves.

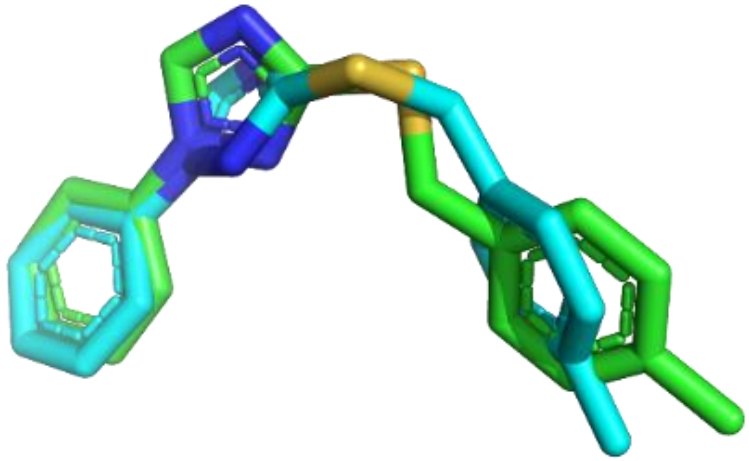

Figure 2. Visualization of the overlap between the native ligand position before (green) and after (blue) *redocking*

Table 1. Redocking results for Lipoxygenase method validation

Grid Box	Validation	
	RMSD (Å)	**ΔG (kcal/mol)**
X = 106.44 Y = 106.44 Z = 106.44	1.913	-9.05

The graphical representation in Figure 2 illustrates a meticulous congruence between the ligand obtained from redocking (depicted in blue) and the initial ligand (illustrated in green). The attainment of this minimal RMSD value substantiates the dependability of the employed flexible docking methodology, thereby establishing a robust and validated computational framework for forecasting molecular interactions of the leaf test compounds from *Jatropha curcas* L. in forthcoming analyses.

2. Molecular docking results

Docking assessments targeted selected secondary metabolites from *Jatropha curcas* L. leaves representing flavonoids, lignans, and glycosides. Structural analysis highlighted the abundance of phenolic hydroxyl (–OH) groups in flavonoid and lignan scaffolds as a key driver of binding [24]. These –OH moieties act as proton donors that strengthen ligand recognition within the active site. Hydrogen bonding networks were predicted to form with important polar residues, including GLU369 and THR431. Such

interactions support stable accommodation of the ligands in the LOX binding pocket.

YASARA based dynamic simulations showed that glycone addition in glycosides does not cause steric hindrance. Glycosylation instead improved overall complex stability [25]. Hydroxyl rich glycone groups enabled additional polar contacts with residues near the pocket periphery. Local side chain flexibility supported these contacts through an induced fit adjustment [26]. Such interactions likely strengthened binding persistence during the simulation.

Thermodynamic results in Table 2 show that all tested ligands produced negative binding energies (ΔG < 0), indicating spontaneous and stable interactions [27]. Glycosides displayed the highest predicted affinities among the compound set. Naringenin 7 O β D glucopyranoside showed the strongest binding energy (–10.41 kcal/mol), followed by Pinoresinol 4′ O β D glucopyranoside (–10.03 kcal/mol) and Buddlenol D (–9.91 kcal/mol). These values surpassed the binding of the native ligand XRP (–9.05 kcal/mol) and the control drug Zileuton (–7.48 kcal/mol).

Conversely, aglycone compounds such as (2S,3S) -Epicatechin (-8.95 kcal/mol) and (-) -Pinoresinol (-8.80 kcal/mol) demonstrate competitive interaction profiles with affinities that are either comparable to or marginally below that of the original ligand. Despite possessing binding energies that are somewhat inferior to those of their glycosidic counterparts, these aglycone compounds nonetheless exhibit remarkably strong and specific interaction potentials at the enzyme's catalytic site

Table 2. Binding energies and interacting residues of test ligands.

PubChem CID	Ligand Name	ΔG (kcal/mol)	Interacting Residues
1778842	XRP (native ligand)	-9.05	HIS378, LEU415, ALA416, ALA606, LEU610, LEU420, VAL603, VAL426, HIS373, GLU369
60490	Zileuton® (control)	-7.48	ARG618, LEU172, TRP109, SER177, TYR408, PHE88, ALA13
92794	Naringenin-7-O-β-D-glucopyranoside	-10.41	LYS175, TRP109, ARG90, ASN173, PHE88, TYR408, ALA13, ARG407, GLU12
486614	Pinoresinol-4′-O-β-D-glucopyranoside	-10.03	ARG145, TYR149, ASP625, GLN108, SER177, TYR408, ARG407, ILE174, ILE403, LEU389, GLU191
157010307	Buddlenol D	-9.91	ALA188, ALA193, ALA416, ALA606, LEU415, LEU419, LEU420, LEU609, LEU610, LYS196, PHE192
162350	Isovitexin	-9.70	ARG145, ASN173, HIS394, TYR107, TYR149, HIS627, TRP109, ALA13
445586343	Syringaresinol-4′-O-β-D-glucopyranoside	-9.13	ASN173, LEU172, LYS175, ASP616, ASP625, ALA179, PHE88, PRO624, ARG618
155320	Chamaejasmin	-9.11	ALA236, LEU326, SER240, LEU658, LEU660, PRO325, GLU234
182232	(2S,3S)-Epicatechin	-8.95	ARG90, GLU12, PHE88, ALA13, TRP109, ASN173
439533	(2R,3R)-Dihydroquercetin	-8.86	ARG618, TRP109, ARG407, ILE403
9064	(2R,3S)-Catechin	-8.82	ARG145, ASP625, TRP109, HIS627, TYR107, ILE403
12309636	(-)-Pinoresinol	-8.80	HIS394, SER177, ASN173, ASP625, TYR408, ARG407, ILE403, LEU389, TRP109, ASP616
12991583	Isoneochamaejasmin A	-8.70	CYS323, GLN319, PRO469, LEU326, PRO325, HIS231, LEU660, VAL659
11604108	(-)-Syringaresinol	-8.62	ARG407, ASP625, THR406, TYR107, PHE88, ALA13, ILE174, ILE403, PHE399, TRP109
21636084	Neochamaejasmin B	-8.59	ARG145, TRP109, VAL117, LEU116, ALA144

Description:
: Hydrogen bonds : *van der Waals* forces : Other bonds
: Hydrophobic interactions : Electrostatic

A comprehensive examination of the molecular interaction dynamics associated with ligands exhibiting optimal affinities is presented in Table 3. In the complex formed between Naringenin-7-O-β-D-glucopyranoside, the stability of bonds is reinforced by an exceptionally intricate network of interactions with residues located in the active site. The principal interactions encompass polar residues ASP625, ASN173, and ARG618, which contribute to the formation of hydrogen and electrostatic bonds [28], alongside aromatic residues PHE88 and TRP109 that enhance hydrophobic stability through stacking interactions [29].

Interaction dynamics involving crucial residues, such as ASP625 and TRP109, are also consistently detected in additional candidate ligands, including (-)-Pinoresinol and (2S,3S)-Epicatechin. These observations elucidate a pattern of conserved interactions at the active sites of LOX enzymes, wherein the residues function as fundamental anchoring points that accommodate a diverse array of ligand structures, encompassing both aglycones and glycosides [30]**.** Naringenin 7 O β D glucopyranoside showed binding energies stronger than both the native ligand XRP and the positive control, supporting its position as the most promising candidate in this study. The main advantage of this ligand is its enhanced thermodynamic inhibition potential, reinforced by an extensive hydrogen bond network [31]. Despite the glycosidic properties posing a challenge to the parameters governing oral bioavailability, the predominant strength of interaction positions it as a priority candidate for subsequent structural optimization, including the modification of the sugar moiety to achieve an equilibrium in its pharmacokinetic profile while maintaining its inhibitory efficacy.

Table 3. Key residues and conserved interaction patterns in the LOX active site.

Residue Name	Dominant Interaction Type	Frequency of Occurrence	Biological Role (Based on Model)
TRP109	Hydrophobic Interaction / π–π Stacking	Dominant (8 of 13 ligands)	Aromatic residue forming the pocket wall, providing an extensive hydrophobic surface for stacking interactions with ligand rings.
ASN173	Hydrogen Bond	High (5 of 13 ligands)	Key polar residue forming hydrogen bond networks, particularly with sugar moieties in glycosides and hydroxyl groups in aglycones.
ARG407	Electrostatic / Hydrogen Bond	High (5 of 13 ligands)	Positively charged residue facilitating ionic interactions or salt bridges with polar ligand groups.
ASP625	Hydrogen Bond / Electrostatic	High (5 of 13 ligands)	Primary proton acceptor interacting with donor groups (such as phenolic -OH) to anchor the ligand orientation.
ILE403	Hydrophobic Interaction (Alkyl)	High (5 of 13 ligands)	Aliphatic residue contributing to the stabilization of the hydrophobic core via Van der Waals forces.
PHE88	Hydrophobic Interaction / π–π Stacking	Moderate (4 of 13 ligands)	Acts synergistically with TRP109 to establish a stable aromatic environment for the ligand.

3. Drug-likeness evaluation using Lipinski's Rule of Five

Physicochemical profiling in Table 4, indicates a clear relationship between predicted oral feasibility and ligand structural class. The category of aglycone compounds, which encompasses monomeric flavonoids (such as Catechin, Epicatechin, Dihydroquercetin) and lignans (including Pinoresinol, Syringaresinol, Buddlenol D), exhibited complete adherence to Lipinski's criteria. These specific compounds possess a molecular weight below 500 Dalton, a moderate logP value (less than 5), and an optimal quantity of hydrogen bond donors and acceptors, which is conducive to passive membrane permeability.

Conversely, the categories of glycoside compounds (for instance, Naringenin-7-O-glucoside and pinoresinol-4'-O-glucoside), along with biflavonoids (such as Chamaejasmin and Neochamaejasmin), consistently fail to meet drug likeness criteria. This shortcoming is primarily attributable to a dual violation regarding the parameters of hydrogen bond donor/acceptor ratios and elevated molecular weight, which arises from the incorporation of sugar moieties or dimeric configurations. These indicate that, despite showing strong inhibition potential in docking, glycosides may face reduced oral bioavailability compared with more drug like aglycone compounds.

Table 4. *Drug-likeness* results based on *Lipinski's Rule of Five*

Ligand Name	Molecular Formula	Parameter					Suitability
		Molecular Weight (<500)	Log P (< 5)	Hydrogen Bond Donor (<5)	Hydrogen Bond Acceptor (<10)	Molar Refractive Index (40-130)	
Buddlenol D	$C_{38}H_{58}O_4$	**578**	**9.69**	1	4	**171.19**	No
(2R,3S)-Catechin	$C_{15}H_{14}O_6$	290	1.55	**5**	6	72.62	Yes
Chamaejasmin	$C_{28}H_{22}O_{12}$	**542**	4.49	**6**	**10**	**138.14**	No
(-)-Syringaresinol	$C_{22}H_{26}O_8$	418	3.21	2	8	106.79	Yes
(2S,3S)-Epicatechin	$C_{15}H_{14}O_6$	290	1.55	**5**	6	72.62	Yes
Isoneochamaejasmin A	$C_{30}H_{22}O_{10}$	**542**	4.49	**6**	**10**	**138.14**	No
Isovitexin	$C_{21}H_{20}O_{10}$	432	0.09	**7**	**10**	105.63	No
Naringenin-7-O-β-D-glucopyranoside	$C_{21}H_{22}O_{10}$	434	-0.02	**6**	**10**	102.93	No
Neochamaejasmin B	$C_{30}H_{22}O_{10}$	**542**	4.49	**6**	**10**	**138.14**	No
(-)-Pinoresinol	$C_{20}H_{22}O_6$	358	3.19	2	6	93.68	Yes
Pinoresinol-4′-O-β-D-glucopyranoside	$C_{26}H_{32}O_{11}$	**520**	0.66	**5**	**11**	126.41	No
Syringaresinol-4′-O-β-D-glucopyranoside	$C_{28}H_{36}O_{13}$	**580**	0.68	**5**	**13**	**139.52**	No
(2R,3R)-Dihydroquercetin	$C_{15}H_{12}O_7$	304	1.19	**5**	7	73.25	Yes

Note: Bold numbers indicate violations of *Lipinski's Rule of Five*

4. ADMET study using pkCSM

The pharmacokinetic characteristics and toxicity of the compound were assessed using in silico methodologies (Table 5). Regarding absorption, the entire test compound demonstrated a satisfactory level of intestinal permeability (greater than 30%) in accordance with established literature criteria. The compound (-)-Pinoresinol demonstrated the highest absorption rate of 93.29%, indicating exceptional oral bioavailability. Conversely, glycoside

derivatives such as Syringaresinol-4′-O-β-D-glucopyranoside exhibited reduced absorption (32.59%), which is marginally above the minimum threshold, attributable to the elevated polarity of the sugar moieties [32]. In terms of associated efflux transporters, the entire compound is categorized as a substrate of P-glycoprotein, which may inhibit the intracellular accumulation of the pharmacological agent.

Regarding distribution, the entire compound exhibited logBB values of less than 0.3 and logPS values of less than -2. This diminished permeability profile concerning the blood-brain barrier is considered a beneficial attribute for peripheral antioxidant agents, as it reduces the likelihood of crossing into the brain parenchyma and minimizes the potential for neurotoxic adverse effects on the central nervous system.

Metabolism predictions identified only two compounds, (–) Pinoresinol and (–) Syringaresinol, as CYP3A4 substrates. This result indicates a potential risk of drug drug interactions if co administered with CYP3A4 inhibitors or inducers. Future studies should consider this possibility during compound prioritization and experimental validation. Other ligands were predicted to show metabolic stability toward CYP3A4 and CYP2D6 isoforms.

Table 5. ADMET analysis of compounds in *Jatropha curcas* L. leaves.

	Absorption		**Distribution**		**Metabolism**		**Excretion**		**Toxicity**	
Compound	**Intestinal Absorption (%)**	**P-gp Substrate**	**BBB Permeability (LogBB)**	**SSP Permeability (Log PS)**	**CYP2D6 Substrate**	**CYP3A4 Substrate**	**Total Clearance (log ml/min/kg)**	**Renal OCT2 Substrate**	**AMES Toxicity**	**Hepatotoxicity**
Syringaresinol-4′-O-β-D-glucopyranoside	78.823	Yes	-0.771	-3.146	No	Yes	0.255	No	No	No
(-)-Syringaresinol	44.376	Yes	-1.903	-4.174	No	Yes	0.377	No	No	No
(-)-Pinoresinol	93.29	Yes	-0.439	-2.975	No	Yes	0.023	No	No	No
Pinoresinol-4′-O-β-D-glucopyranoside	53.365	Yes	-1.485	-4.003	No	Yes	0.39	No	No	No
Buddlenol D	77.285	Yes	-2.031	-4.07	No	No	0.521	No	No	No
(2R,3R)-Dihydroquercetin	64.709	Yes	-0.725	-3.198	No	No	-0.078	No	No	No
(2S,3S)-Epicatechin	68.829	Yes	-1.054	-3.298	No	No	0.183	No	No	No
(2R,3S)-Catechin	68.829	Yes	-1.054	-3.298	No	No	0.183	No	No	No
Isovitexin	64.729	Yes	-1.375	-3.754	No	No	0.442	No	No	No
Naringenin-7-O-β-D-glucopyranoside	36.035	Yes	-1.261	-4.053	No	No	0.378	No	No	No
Chamaejasmin	81.124	Yes	-1.035	-3.216	No	No	-0.23	No	No	No
Neochamaejasmin B	81.124	Yes	-1.035	-3.216	No	No	-0.23	No	No	No
Isoneochamaejasmin A	81.124	Yes	-1.035	-3.216	No	No	-0.23	No	No	No
Grade requirement	**≥ 30**	**-**	**> 0.3**	**≥ -2**	**-**	**-**	**Higher is better**	**-**	**-**	**-**

All compounds are anticipated to exhibit low to moderate rates of total clearance and a minimal likelihood of renal excretion via the organic cation transporter 2 (OCT2). Regarding toxicological assessment, neither compound is expected

to possess mutagenic properties (negative Ames test) or hepatotoxicity. Nevertheless, it is essential to emphasize that these findings are derived from computational model estimations; therefore, ongoing validation through in vitro toxicity assays is crucial to ascertain the safety profile of the compound unequivocally.

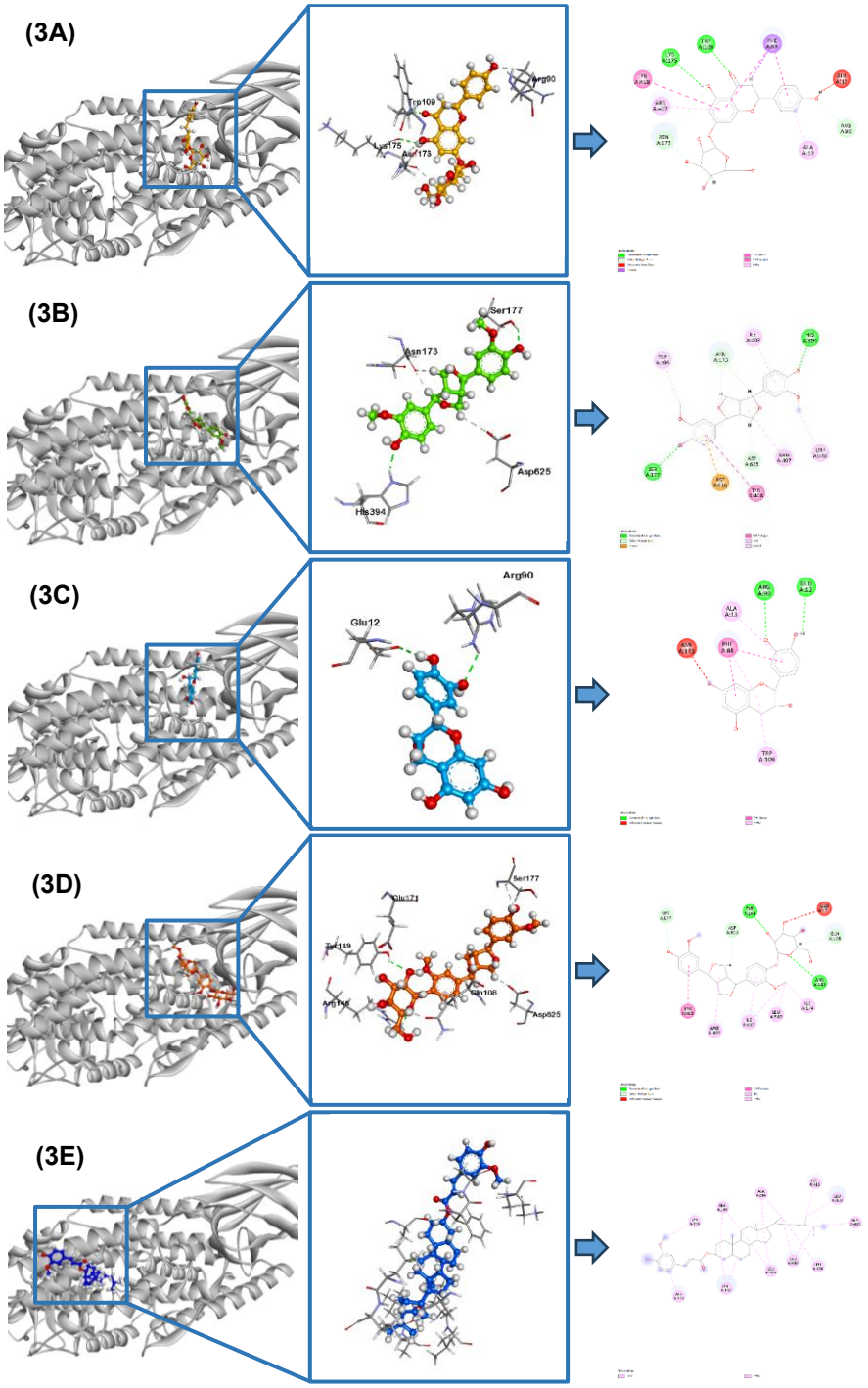

Figure 3. 3D binding modes of top *J. curcas* ligands within the Lipoxygenase active site (PDB: 7LAF). **(A)** Naringenin-7-O-β-D-glucopyranoside (highest affinity); **(B)** (-)-Pinoresinol (optimal oral candidate); **(C)** (2S,3S)-Epicatechin; **(D)** Pinoresinol-4′-O-β-D-glucopyranoside; **(E)** Buddlenol D. Ligands are rendered as sticks; dotted lines indicate hydrogen bonds and hydrophobic contacts.

5. Ligand-Protein Complex Visualization

Five representative ligands were selected for detailed binding mode analysis in (Figure 3) based on two criteria: (1) Maximum Inhibition Potential, represented by high-affinity compounds (e.g., Naringenin-7-O-β-D-glucopyranoside, Buddlenol D, and (2) Oral Drug Candidate Profile, represented by aglycones balancing affinity with Lipinski compliance (e.g., (-)-Pinoresinol). Visualization panels display the 3D binding orientation (left), specific molecular interactions (center), and comprehensive 2D residue maps (right).

Structural analysis of glycosides (Figures 3A, 3D) reveals that the sugar moiety stabilizes the complex via extensive hydrogen bond networks with polar residues at the pocket's lip (ASN173, ARG618, ASP625). This polar interaction acts as a secondary anchor, explaining the superior affinity of glycosides (-10.41 and -10.03 kcal/mol) despite their larger volume. Conversely, aglycones (Figures 3B, 3C) penetrate deeper into the hydrophobic pocket, stabilized by π–π stacking with conserved residues PHE88 and TRP109, alongside H-bonds with ASP625 and ARG407.

Uniquely, Buddlenol D (Figure 3E) lacks classical hydrogen bonds, relying instead on extensive hydrophobic and Van der Waals contacts to achieve high affinity (-9.91 kcal/mol), underscoring the role of dispersion forces. The consistent interaction of ASP625 and TRP109 across these ligands identifies them as critical anchoring points, suggesting that targeting these residues is a rational strategy for optimizing future LOX inhibitors.

CONCLUSION

Flexible molecular docking using YASARA indicated that bioactive compounds from *Jatropha curcas* L. leaves have potential antioxidant activity through inhibition of Lipoxygenase (LOX). Naringenin 7 O β D glucopyranoside showed the strongest predicted binding affinity (ΔG = −10.41 kcal/mol), outperforming both the native ligand and the positive control, Zileuton (ΔG = −7.48 kcal/mol). This high affinity was supported by an extensive hydrogen bonding network, particularly involving ASN173 and ARG618. (−) Pinoresinol and (2S,3S) Epicatechin also exhibited favorable interactions, reinforced by conserved hydrophobic contacts with PHE88 and TRP109. Pharmacokinetic screening identified (−) Pinoresinol as the most promising oral candidate due to full compliance with Lipinski criteria and a more favorable ADMET profile. These findings provide a structure based rationale for prioritizing *Jatropha curcas* derived compounds as LOX inhibitor candidates and support further validation through in vitro assays.

REFERENCES

[1] N. Chandimali *et al.*, “Free radicals and their impact on health and antioxidant defenses: a review,” *Cell Death Discov.*, vol. 11, no. 1, p. 19, 2025, doi: 10.1038/s41420-024-02278-8.

[2] P. Rajak *et al*., "In silico targeting of lipoxygenase, CYP2C9, and NAD(P)H oxidase by major green tea polyphenols to subvert oxidative stress," *Adv. Redox Res.*, vol. 7, p. 100061, 2023, doi: 10.1016/j.arres.2023.100061.

[3] İ. Gulcin, "Antioxidants: a comprehensive review," *Arch. Toxicol.*, vol. 99, no. 5, pp. 1893–1997, May 2025, doi: 10.1007/s00204-025-03997-2.

[4] S. A. B. Galal, M. Madhat Mousa, E. S. Elzanfaly, E. M. Hussien, E. A. H. Amer, and H. E. Zaazaa, "Quantitative analysis of residual butylated hydroxytoluene and butylated hydroxyanisole in *Salmo salar*, milk, and butter by liquid chromatography–tandem mass spectrometry," *Food Chem.*, vol. 453, p. 139653, 2024, doi: 10.1016/j.foodchem.2024.139653.

[5] L. Méndez, J. Rojas, C. Izaguirre, B. Contreras, and R. Gómez, "*Jatropha curcas* leaves analysis reveals it as mineral source for low sodium diets," *Food Chem.*, vol. 165, pp. 575–577, 2014, doi: 10.1016/j.foodchem.2014.05.124.

[6] S. Rahman, E. P. Toepak, and S. C. Angga, "Uji aktivitas antioksidan dan sitotoksik ekstrak daun Jarak Pagar (*Jatropha curcas*)," *Jurnal SAGO Gizi dan Kesehatan*, vol. 4, no. 2, pp. 239–244, 2023, doi: 10.30867/gikes.v4i2.1175.

[7] S. Yakubu and G. Yebpella, "Antioxidant activity of bioactive and mineral constituents of *Jatropha curcas* Linn. (Euphorbiaceae) leaf and seed extract," *J. Chem. Nat. Resour.*, vol. 6, pp. 1–9, May 2024, doi: 10.32734/jcnar.v6i1.15658.

[8] M. Lončarić, I. Strelec, T. Moslavac, D. Šubarić, V. Pavić, and M. Molnar, "Lipoxygenase inhibition by plant extracts," *Biomolecules*, vol. 11, no. 2, Feb. 2021, doi: 10.3390/biom11020152.

[9] H. Slika *et al*., "Therapeutic potential of flavonoids in cancer: ROS-mediated mechanisms," *Biomed. Pharmacother.*, vol. 146, p. 112442, Feb. 2022, doi: 10.1016/j.biopha.2021.112442.

[10] K. N. Hemavathi, S. Skariyachan, R. Raju, T. S. Keshava Prasad, and C. S. Abhinand, "Computational screening of potential anti-inflammatory leads from Jeevaneeya Rasayana plants targeting COX-2 and 5-LOX by molecular docking and dynamic simulation approaches," *Comput. Biol. Med.*, vol. 171, p. 108164, 2024, doi: 10.1016/j.compbiomed.2024.108164.

[11] G. Zengin *et al*., "Chemical composition and biological properties of two *Jatropha* species: Different parts and different extraction methods," *Antioxidants*, vol. 10, no. 5, p. 792, 2021, doi: 10.3390/antiox10050792.

[12] Y. Wang *et al*., "Chemical constituents

from leaves of *Jatropha curcas*," *Chinese Herb. Med.*, vol. 15, no. 3, pp. 463–469, 2023, doi: 10.1016/j.chmed.2022.08.010.

[13] E. Navarrete *et al.*, "Development of ferrocenyl and ruthenocenyl zileuton analogs with enhanced bioactivity toward human 5-lipoxygenase: Innovation in drugs for inflammatory diseases," *Inorg. Chem.*, vol. 64, no. 7, pp. 3495–3505, Feb. 2025, doi: 10.1021/acs.inorgchem.4c05103.

[14] E. Krieger and G. Vriend, "Increasing the precision of comparative models with YASARA NOVA: A self-parameterizing force field," *Proteins: Struct. Funct. Bioinf.*, vol. 47, no. 3, pp. 393–402, 2002, doi: 10.1002/prot.10104.

[15] T. A. Nyijime *et al.*, "Computational design, pharmacokinetics, molecular docking and molecular dynamic simulation of novel anti-tubercular inhibitors," *Silico Res. Biomed.*, vol. 1, p. 100012, 2025, doi: 10.1016/j.insi.2025.100012.

[16] H. Land and M. S. Humble, "YASARA: A tool to obtain structural guidance in biocatalytic investigations," in *Protein Engineering: Methods and Protocols*, U. T. Bornscheuer and M. Höhne, Eds. New York, NY, USA: Springer, 2018, pp. 43–67, doi: 10.1007/978-1-4939-7366-8_4.

[17] E. J. Millan-Casarrubias, Y. V. García-Tejeda, C. H. González-De la Rosa, L. Ruiz-Mazón, Y. M. Hernández-Rodríguez, and O. E. Cigarroa-Mayorga, "Molecular docking and pharmacological in silico evaluation of camptothecin and related ligands as promising HER2-targeted therapies for breast cancer," *Curr. Issues Mol. Biol.*, vol. 47, no. 3, p. 193, 2025, doi: 10.3390/cimb47030193.

[18] C. A. Lipinski, F. Lombardo, B. W. Dominy, and P. J. Feeney, "Experimental and computational approaches to estimate solubility and permeability in drug discovery and development settings," *Adv. Drug Deliv. Rev.*, vol. 46, no. 1, pp. 3–26, 2001, doi: 10.1016/S0169-409X(00)00129-0.

[19] D. E. V. Pires, T. L. Blundell, and D. B. Ascher, "pkCSM: Predicting small-molecule pharmacokinetic and toxicity properties using graph-based signatures," *J. Med. Chem.*, vol. 58, no. 9, pp. 4066–4072, May 2015, doi: 10.1021/acs.jmedchem.5b00104.

[20] F. Wu *et al.*, "Computational approaches in preclinical studies on drug discovery and development," *Front. Chem.*, vol. 8, p. 726, 2020, doi: 10.3389/fchem.2020.00726.

[21] J. P. B. Arango, D. Y. M. Rodriguez, S. L. Cruz, and G. T. Ocampo, "In silico evaluation of pharmacokinetic properties and molecular docking for the identification of potential anticancer compounds," *Comput. Biol. Chem.*, vol. 120, p. 108626, 2026, doi:

10.1016/j.compbiolchem.2025.108626.

[22] W.-C. Tsai *et al.*, "Kinetic and structural investigations of novel inhibitors of human epithelial 15-lipoxygenase-2," *Bioorg. Med. Chem.*, vol. 46, p. 116349, 2021, doi: 10.1016/j.bmc.2021.116349.

[23] H. Rimac, M. Grishina, and V. Potemkin, "Use of the complementarity principle in docking procedures: A new approach for evaluating the correctness of binding poses," *J. Chem. Inf. Model.*, vol. 61, no. 4, pp. 1801–1813, Apr. 2021, doi: 10.1021/acs.jcim.0c01382.

[24] M. K. Mandal, W. Gan, and A. J. Domb, "Phenolate-based bioactive compounds: Design, delivery and biomedical applications," *Coord. Chem. Rev.*, vol. 544, p. 216941, 2025, doi: 10.1016/j.ccr.2025.216941.

[25] H. Zhang *et al.*, "Molecular mechanisms underlying the absorption of aglycone and glycosidic flavonoids in a Caco-2 BBe1 cell model," *ACS Omega*, vol. 5, no. 19, pp. 10782–10793, May 2020, doi: 10.1021/acsomega.0c00379.

[26] A. Chen, Z. Jiang, and M. D. Burkart, "Enzymology of standalone elongating ketosynthases," *Chem. Sci.*, vol. 13, no. 15, pp. 4225–4238, 2022, doi: 10.1039/D1SC07256K.

[27] Y. Wang, J. Li, X. Li, B. Gao, J. Chen, and Y. Song, "Spectroscopic and molecular docking studies on binding interactions of camptothecin drugs with bovine serum albumin," *Sci. Rep.*, vol. 15, no. 1, p. 8055, 2025, doi: 10.1038/s41598-025-92607-3.

[28] H. Meuzelaar, J. Vreede, and S. Woutersen, "Influence of Glu/Arg, Asp/Arg, and Glu/Lys salt bridges on α-helical stability and folding kinetics," *Biophys. J.*, vol. 110, no. 11, pp. 2328–2341, Jun. 2016, doi: 10.1016/j.bpj.2016.04.015.

[29] R. Calinsky and Y. Levy, "Aromatic residues in proteins: Re-evaluating the geometry and energetics of π–π, cation–π, and CH–π interactions," *J. Phys. Chem. B*, vol. 128, no. 36, pp. 8687–8700, Sep. 2024, doi: 10.1021/acs.jpcb.4c04774.

[30] R. Laczko and K. Csiszar, "Lysyl oxidase (LOX): Functional contributions to signaling pathways," *Biomolecules*, vol. 10, no. 8, Aug. 2020, doi: 10.3390/biom10081093.

[31] V. S. Shilpa *et al.*, "Phytochemical properties, extraction, and pharmacological benefits of naringin: A review," *Molecules*, vol. 28, no. 15, Jul. 2023, doi: 10.3390/molecules28155623.

[32] L. Guo, J. Qiao, J. Huo, and H. P. V. Rupasinghe, "Plant iridoids: Chemistry, dietary sources and potential health benefits," *Food Chem. X*, vol. 27, p. 102491, 2025, doi: 10.1016/j.fochx.2025.102491.